ISSN: 2579-5821 (Print)
ISSN: 2579-5546 (Online)
URL address: http://journal.unhas.ac.id/index.php/geocelebes
DOI: 10.70561/geocelebes.v9i1.40206

Jurnal Geocelebes Vol. 9 No. 1, April 2025, 15 – 27

Analysis of Landslide Hazard Levels on the Palopo – Luwu Road using GIS and Finite Element Method

Anshar Abdullah Jawil*, Kadek Nando Setiawan

Department of Mining Engineering, University Andi Djemma, Palopo 91922, Indonesia.

*Corresponding author. Email: anshar@unanda.ac.id

Manuscript received: 23 September 2024; Received in revised form: 6 March 2025; Accepted: 23 April 2025

Abstract

Indonesia is one of the countries that often experiences landslides during the rainy season. The Palopo–Luwu main road is a landslide-prone area in North Bastem sub-district because it has a topographic condition with a very steep slope. Therefore, it is important to conduct research on the analysis of the potential for landslides in the area. The method used in this study is Weighted Overlay based on Geographic Information Systems (GIS) in making landslide-prone maps. Data processing with weighting or scoring on parameters such as slope, rainfall, rock type, soil type, and land cover. While the Finite Element Method (FEM) is used to model slope stability with input data on physical and mechanical properties of rocks and slope geometry data as a basis for calculating the slope safety factor (FK). The results of the study showed that almost 85% of the research area is a high landslide potential area which is the Palopo–Luwu main road area, this was validated from laboratory test data which was then analyzed for slope stability showing FK value <1.25, which is 0.936 and the actual condition of the slope in the field has collapsed. The mapping results can be used as a useful tool for land use planning and risk reduction in the research area.

Keywords: FEM; FK; GIS; landslide; weighted overlay.

Citation: Jawil, A. A., & Setiawan, K. N. (2025). Analysis of Landslide Hazard Levels on the Palopo – Luwu Road using GIS and Finite Element Method. *Jurnal Geocelebes*, 9(1): 15–27, doi: 10.70561/geocelebes.v9i1.40206

Introduction

Indonesia is one of the countries that often experiences landslides during the rainy season (Susilo et al., 2020). A landslide is the movement of earthen materials down a slope under the influence of gravity and occurs when earthen material exceeds the shear strength (Pawluszek et al., 2020; Jawil & Pontus, 2023). landslides can be regarded as one of the most frequent geological hazards in mountainous areas (Chen & Zhang, 2021). Researchers found the factors most important for landslides to be geological and geomorphological conditions, precipitation, in addition to disturbances due to human activity playing an important role in the occurrence of landslides (Neamat & Karimi, 2020). Landslide disasters can result in loss of biodiversity, human lives, property, and damage to infrastructure (Saleem at al., 2020). Luwu Regency is one of the regencies that has the potential to be prone to landslides. According to disaster data from South Sulawesi Province, there have been 18 landslides in Luwu Regency since July 2021, while in North Bastem District itself, there have been 3 landslides since 2023. One of the recent landslide disasters occurred on February 26, 2024 on the Palopo-Luwu main road, which killed 5 residents and cut off access to the intercity road.

The high incidence of landslides in the North Bastem area, which is the only traffic route between Palopo City and Luwu Regency, requires research on the analysis of the potential for landslides, especially in the Palopo–Luwu main road area. Therefore, it is important to conduct research with a combination of several methods to obtain more accurate results in predicting or modeling the landslide potential of an area.

Advances in information and communication technology are developing very rapidly, especially Geographic Information Systems (GIS). This system can be used to analyze disaster risks by considering spatial data in more detail. GIS is considered an efficient and cost-effective technology that can display a large set of geographically referenced data, by combining physical processes and disaster-causing factors (Wang et al., 2020). The results of landslide vulnerability mapping are then validated with the results of slope stability analysis using FEM (Finite Element Method). The safety factor (FK) value is used to ensure that the slope is in a safe condition. The safety factor value is obtained from the comparison of the total retaining force to the force that causes the slope to collapse. The combination of these two methods is used to obtain spatial information. The results of laboratory testing are used for slope stability modeling which strengthens the results of spatial landslide potential mapping. This is very important to do to get an initial picture of the areas that are included in the Red Zone and still have a high level of landslide potential.

The FEM stress-strain assessments are usually applied to evaluate the landslide body's progressive failure as well as to introduce initial velocity and later acceleration up to the moment major deformations are observed in the slope and computational convergence is achieved (Cuomo et al., 2021). FEM has been reported to be more effective for slope stability analysis (Chen et al., 2019). This is observed by Li et al. (2016), due to the considerable reduction in the number of analyses required in the calculation process which subsequently leads to an improvement in computational efficiency at low probability levels and this is important in slope design practice. The approach proposed in this study allows the utilization of information obtained from a simple method (GIS) in a more advanced model, FEM, to ensure reliability

Materials and Methods

Collecting Data

The data collection used is primary data and secondary data. Primary data is data obtained from direct measurements in the field, such as rock samples and slope geometry (Figure 1). Field investigations are conducted to determine field conditions by taking documentation photos of slope conditions, geology, and vegetation (Figure 2). While secondary data is obtained from several related agencies and official government sites such as land use maps, soil types, geological conditions, rainfall, and topographic data of the research area.

Figure 1. (left) Measurement of slope geometry, and (right) Soil Sampling.

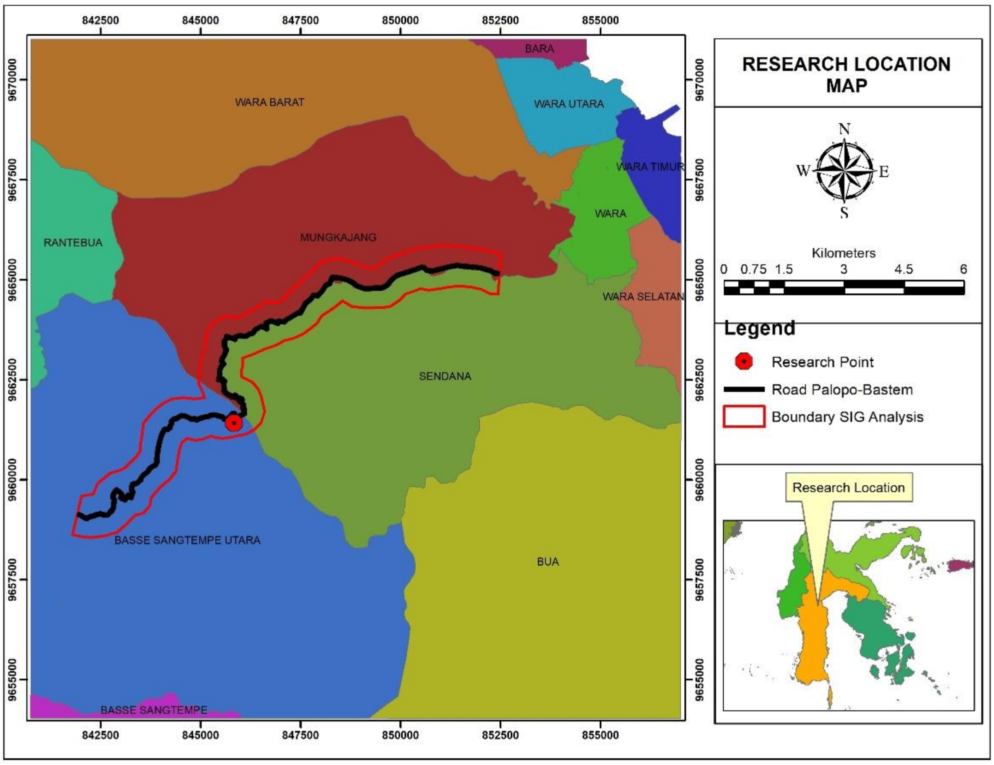

Figure 2. Research location map.

Data Processing and Laboratory Testing

The method used in making landslide susceptibility maps is Weighted Overlay. This technique combines the weighting of each parameter and the scoring of each parameter class (Khatun et al., 2023). Then the rainfall map, rock type map, soil type map, land cover map are overlaid to get an overview of the landslide level in the research area. Laboratory tests were conducted on 10 rock samples to obtain rock property values including physical properties (unique weight and water content) and mechanical properties (cohesion and friction angle). The results of laboratory analysis were used as input for rock layer property values. slope stability modeling using the FEM.

Direct shear test includes determining the shear strength of consolidated drained and consolidated undrained soil materials in a direct shear test. This test is carried out by forming a specimen which is then passed through a shear test equipment media with a loading speed that can be adjusted (Du et al., 2021). FEM is a method of analyzing rock/soil slopes that are divided into several small block zones, in this research model it is divided into 4,500 number of surfaces computed (Pilecka et al., 2022). Elements in a reduced zone are connected by node points. The analysis involves calculating displacements at each node, then using interpolation functions (shape functions) to estimate stresses and strains within elements (Brady & Brown, 2006). The factor of safety (FK) is derived from these computations using slope modeling software.

The Bishop method is used to analyze the slip surface. In this method, it is assumed that the total normal forces are located/ working at the center of the base of the section and can be determined by decomposing the forces on the section vertically or normally (Nath et al., 2021). Equilibrium requirements are applied to the sections that form the slope. The Bishop method assumes that the forces acting on the section have a zero resultant in the vertical direction. This method reduces the shear strength to describe the slope failure, so the value obtained from this approach is used as a safety factor.

Data analysis

Data analysis was carried out by comparing the results of landslide disaster potential mapping using GIS and the results of slope stability modeling using FEM, the classification of landslide vulnerability levels will be confirmed by the slope safety factor value from the modeling input with field data. Slope stability modeling also conducted sensitivity analysis on the input rock material properties. The parameters used in landslide vulnerability mapping are slope gradient, rainfall, rock type, soil type, and land cover. The percentage of indicator weight of each parameter refers to PU Regulation No. 22 of 2007.

Results and Discussion

Land Slope

The slope of the research area is divided into 5 classes with 90% of the area being dominated by slopes above 25% (Figure 3). This defines that the research area is a steep topography. The main road of Palopo–Luwu crosses between the steep cliffs. Steep slopes or cliffs will increase the driving force. Steep slopes are formed due to erosion by river water, springs, sea water, and wind.

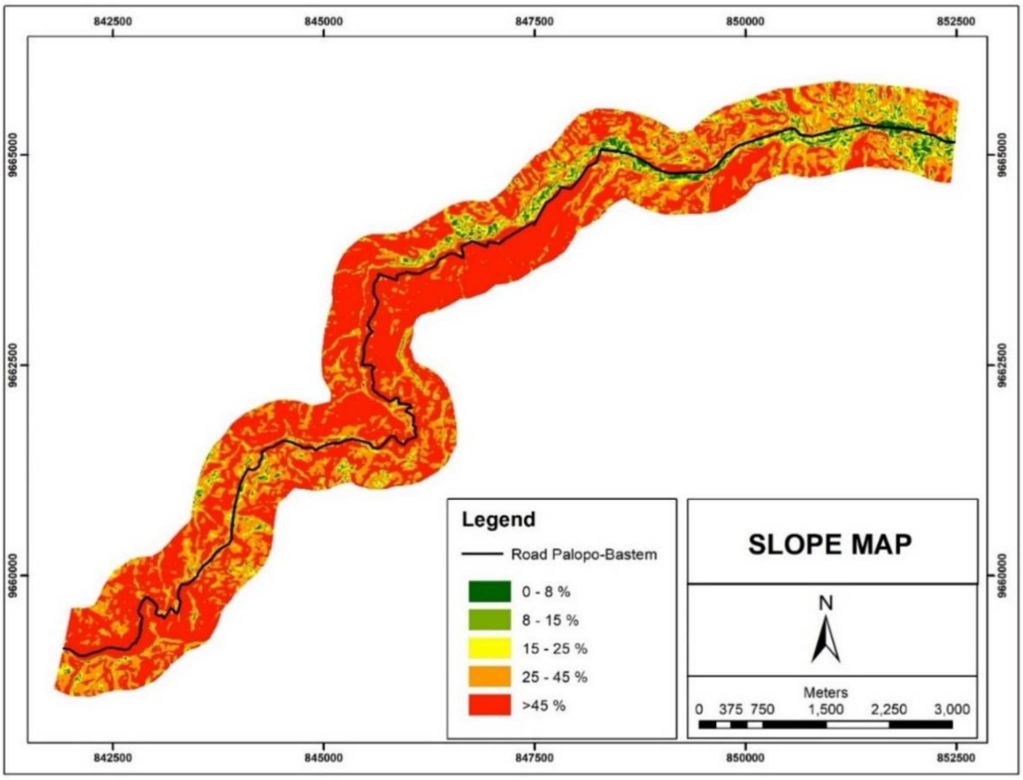

Figure 3. Land slope classification.

Table 1. Land slope classification.

Slope %	Weight	Score
>45		5
30-45		4
15-30	20%	3
8-15		2
<8		1

Land slope has a weight of 20% with the highest score being 5 for land slopes above 45% (Table 1). According to Rawat & Pant (2023), land with a slope of more than 45% has greater potential compared to land with a slope below 45%. The steep slope of the land also causes the runoff water to flow quickly, which can cause erosion which is an early symptom of landslides.

Rainfall

The research area is a plateau, so the rainfall in the area is quite high, that is 3000 - 3500 mm/year included in a very wet area with an assessment score of 5 (Figure 4). The rainfall factor has a weight of 30% (PU Regulation No. 22 of 2007). High rainfall can be a supporting factor for landslides (Liu et al., 2021). In mountain regions, landslides are often triggered by intensive rainfall. Rainfall and infiltration enhance moisture content, which further decreases the matrix suction and soil shear strength (Huang et al., 2021). According to Liu (2021), landslides were triggered by rainfall of a certain intensity and, according to the results obtained from the present tests, the rainfall intensity must exceed 40 mm/h to trigger a landslide.

A long dry season will cause large amounts of water to evaporate on the surface of the soil. Pores or cavities in the soil will appear, then cracks and fissures will occur on the surface. When it rains, water will seep into the cracked parts. The soil will quickly expand again. At the beginning of the rainy season, the water content in the soil becomes saturated in a short time. Heavy rain at the beginning of the season can cause landslides because through the cracked soil, water will enter and accumulate at the base of the slope, causing lateral movement. If there are trees on the surface, landslides can be prevented because the water will be absorbed by the plants. Plant roots also function as soil binders.

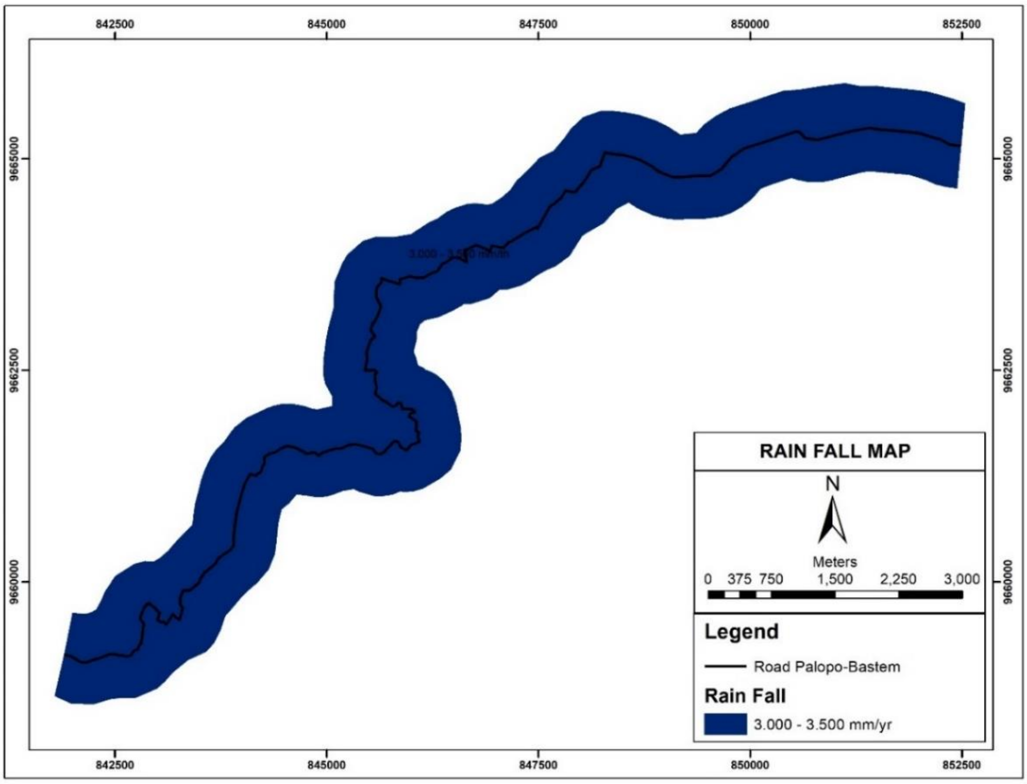

Figure 4. Rain fall map.

Rock Type

The nature of each rock is different, it depends on the origin of the formation of the rock. In general, rocks are influenced by texture, structure, fracture, mineral content, weather, and sedimentation. Morphologically, the area in the Malili sheet is divided into 4 units, which are Mountainous Area, Hilly Area, Karst Area, and Plains Area (Simandjuntak et al., 2007). The mountainous area occupies the western - southeastern part of the Malili sheet. The Hilly Area occupies the central to northeastern part of the Malili sheet, with an altitude between 200 – 700 meters above sea level. The Karst Region occupies the northeastern part of the Malili sheet, with an elevation ranging between 800–1700 meters above sea level (masl), formed by limestone. The Lowland Region covers the southern part of the Malili sheet, stretching from north of Palopo, Sabbang, and Masamba to Bone-Bone.

The Majene Sheet and the Western Part of the Palopo Sheet are formed by various types of rocks such as sedimentary, metamorphic, volcanic, and intrusive rocks. Their ages range from Mesozoic to Quaternary. The oldest unit in this Sheet is Metamorphic Rock (TRw) which consists of schist, genes, phyllite and slate. This unit may be equated with the Wana Complex in the Pasangkayu Sheet which is thought to be older and Cretaceous and is overlain unconformably by the Latimojong Formation (Kls). The formation is composed of phyllite, quartzite, metamorphic mudstone, and marble, of Cretaceous age (Figure 5).

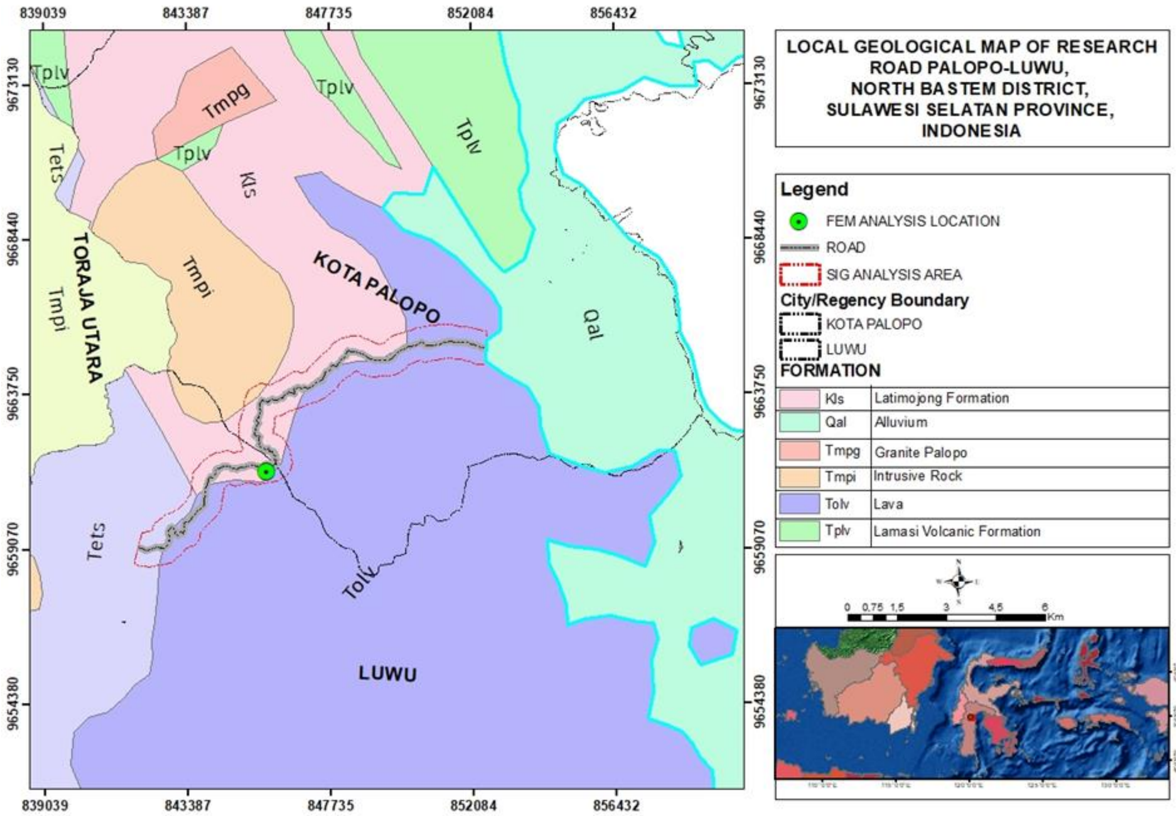

Figure 5. Geological map (modified from Simandjuntak et al., 2007).

Table 2. Rock type classification.

Rock Type	Weight	Score
Alluvial Plain		1
Alluvial Plain (lava)		1
Granite Hills	20%	3
Limestone Hills		2
Limestone Hills (shale)		2

In the research area there are 5 types of rocks, that is alluvial plains, alluvial plains (lava), granite hills, limestone hills, and limestone hills (shale) (Figure 6 and Table 2). The research area is dominated by limestone hills with an area of 0.128 km^2, alluvial plains with an area of 0.123 km^2 and granite hills with an area of 0.025 km^2. In general, volcanic sedimentary rocks and sedimentary rocks are sand-sized and a mixture of gravel, sand, and clay is less strong. These rocks will easily become soil if they experience a weathering process and are generally susceptible to landslides if they are on steep slopes.

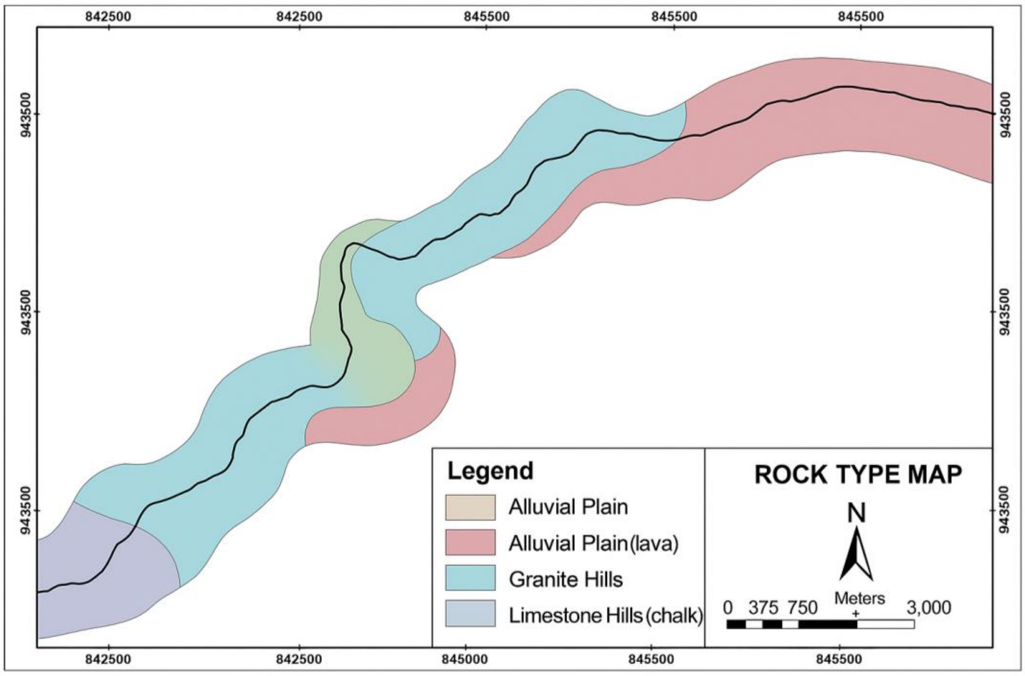

Figure 6. Rock type classification.

Soil Type

The types of soil in the research area are divided into 3, that is alluvial with a score of 1, regosol (ferric arcrisols) and regosol (orthic arcrisols) with a score of 5 (Figure 7). The specific gravity of the soil contributes 15% (Table 3).

Table 3. Soil Type Classification

Soil Type	Weight	Score
Aluvial	15%	1
Regosol (ferric arcrisols)		5
Regosol (Orthic Arcrisols)		5

Land Cover

Table 4. Land cover classification.

Land Cover	Weight	Score
Thicket	15%	4
Dry Forest		3
Settlement		2

Land cover in the research area is divided into three areas (Table 4), that is the thicket area is the largest area, that is 96%, while the residential area and dry land forest are around 4% (Figure 8).

Landslide Potential Map

Based on the results of the total score analysis of the parameters at the research location, 3 landslide vulnerability class classifications were obtained, that is low, medium, and high potential. The high landslide potential area is 372 hectares (42.4%), medium potential is 371 hectares (42.3%) and low potential is 134 hectares (15.2%). The vulnerability level of the landslide potential zone is high if the total weighted value is in the range of 2.40 - 3.00, the vulnerability level is medium if the total weighted value is in the range of 1.70 - 2.39, the vulnerability level is low if the total weighted value is in the range of 1.00 - 1.69. The assessment of the vulnerability level of a landslide potential zone is carried out by adding the weighted values of 5 (five) indicators of slope, rainfall, rock type, soil type, and type of land cover is 134 hectares (15.2%) (Figure 9).

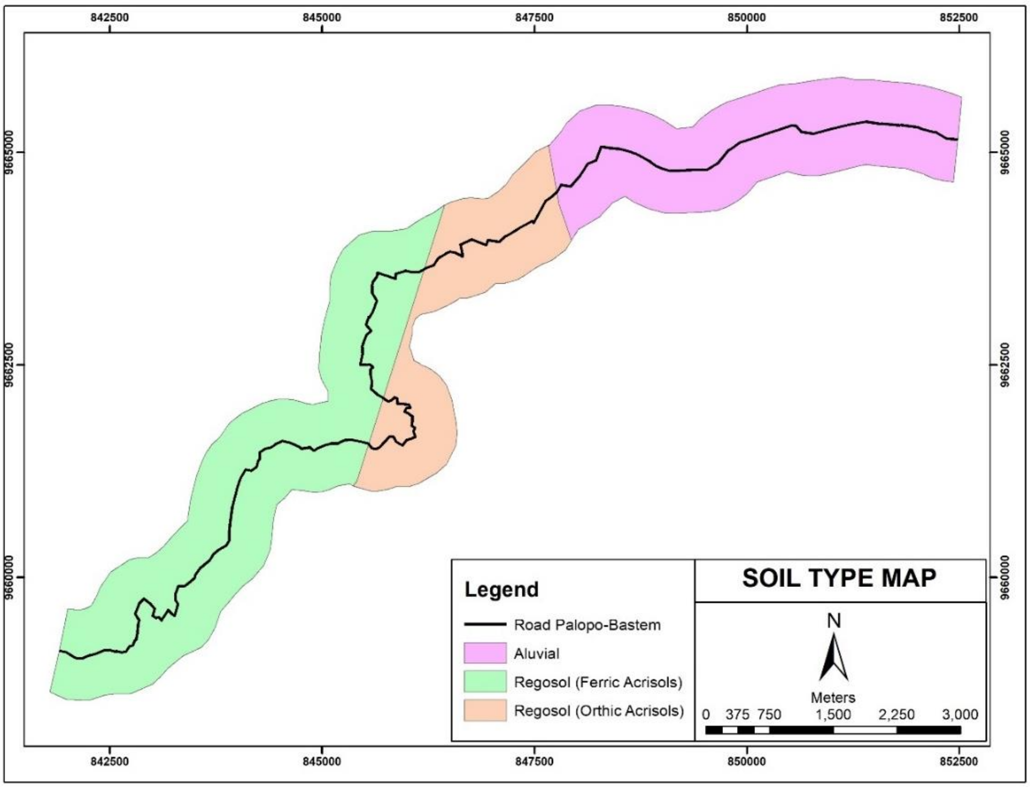

Figure 7. Soil type classification.

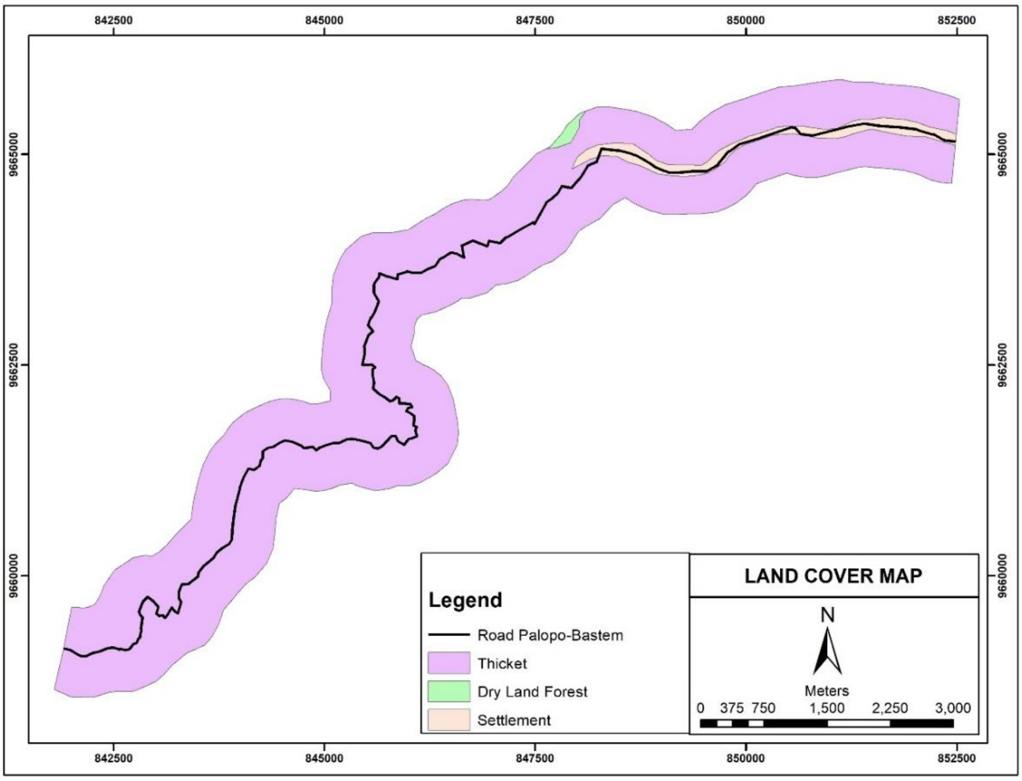

Figure 8. Land Cover Classification

These results show that almost 85% of the research area is an area with a high level of landslide s, which is a concern in carrying out prevention or monitoring in at the red zone points of the Palopo–Luwu main road.

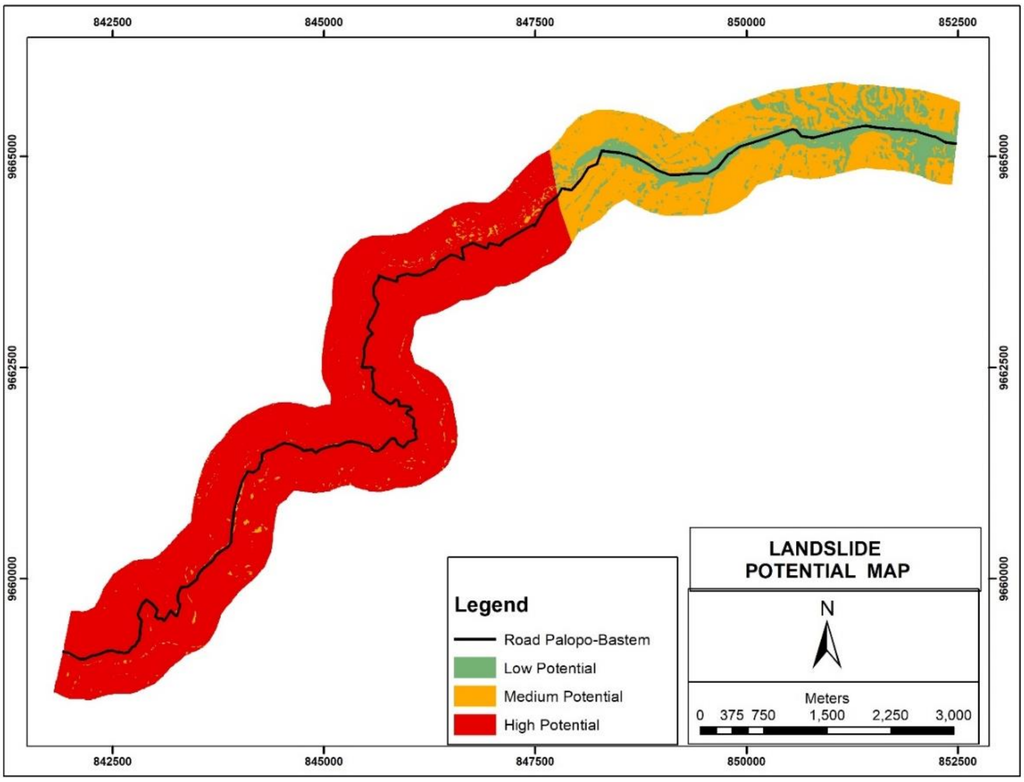

Figure 9. Landslide potential map.

Testing of Physical and Mechanical Properties of Rocks

From the results of laboratory testing of the physical properties of soil samples in the research area, the values of water content, wet soil density, dry soil density were obtained, while the mechanical properties test was in the form of cohesion values and friction angles in the topsoil layer. The test results of 10 soil samples have a cohesion value of 0.325 - 0.701 kg/m^3 and an internal friction angle of 30 - 42 degrees (Table 5).

Table 5. Direct shear strength test.

ID	Easting	Northing	Cohesion	Natural Angle of Repose
LR1-01	844,109.214	9,662,057.656	0.626	40
LR1-02	844,108.612	9,662,051.532	0.350	37
LR2-01	844,109.214	9,662,057.656	0.350	40
LR2-02	844,109.318	9,662,057.677	0.525	39
LR3-01	844,083.856	9,662,077.134	0.701	39
LR3-02	844,083.917	9,662,077.398	0.701	39
LR4-01	844,079.918	9,662,079.513	0.325	30
LR4-02	844,079.965	9,662,079.422	0.601	42
LR5-01	844,086.201	9,662,071.984	0.400	40
LR5-02	844,009.432	9,662,079.167	0.400	35

The water content in the soil samples ranges from 12.05% - 33.90%, the wet weight ranges from 1.54 - 2.03 gr/cm^3 and the dry weight is 1.21 - 1.80 gr/cm^3 (Table 6).

Based on field observations, the layer beneath the soil consists of weathered shale, underlain by basalt rock. The determination of uniaxial compressive strength (UCS) values for the weathered shale and basalt in the field refers to the rock and soil strength classification guidelines (Wyllie & Mah, 2004).

Field observations indicate that the weathered shale falls into the 'Easily scraped by a fingernail (S5)' category, with an estimated UCS range of 3 MPa. Meanwhile, the basalt is classified as 'Hard rock - requires a single hammer blow to fracture (R4),' yielding an estimated UCS of 60 MPa.

These field observations were used to estimate the mi, GSI, and disturbance factor values for both the weathered shale and basalt. Subsequently, the cohesion and internal friction angle values were employed to determine and the results of which are presented in Table 7 (Hoek & Brown, 2019).

Table 6. Water content and density test.

ID	Long	Lat	Average Moisture Content	Wet Density	Dry Density
LR1-01	844,109.214	9,662,057.656	12.43	2,029	1,805
LR1-02	844,108.612	9,662,051.532	12.05	1,617	1,443
LR2-01	844,109.214	9,662,057.656	12.90	1,629	1,443
LR2-02	844,109.318	9,662,057.677	15.94	1,797	1,550
LR3-01	844,083.856	9,662,077.134	27.41	1,618	1,270
LR3-02	844,083.917	9,662,077.398	17.82	1,859	1,578
LR4-01	844,079.918	9,662,079.513	32.34	1,605	1,213
LR4-02	844,079.965	9,662,794.227	25.80	1,765	1,403
LR5-01	844,086.201	9,662,071.984	24.08	1,540	1,242
LR5-02	844,009.432	9,662,079.167	33.90	1,688	1,261

Table 7. Hoek and Brown classification (Hoek & Brown, 2019).

Hoek and Brown Classification		Weathered Layer	Basalt Bed Rock
UCS of Intact Rock	sigci	3 Mpa	60 Mpa
Geological Strength Index	GSI	10	30
Material constant	m_i	25	25
Disturbance Factor	D	0	0
Mohr-Coulomb Fit			
Cohesion	C	0.043	0.031
Friction	phi	31.97	57.28

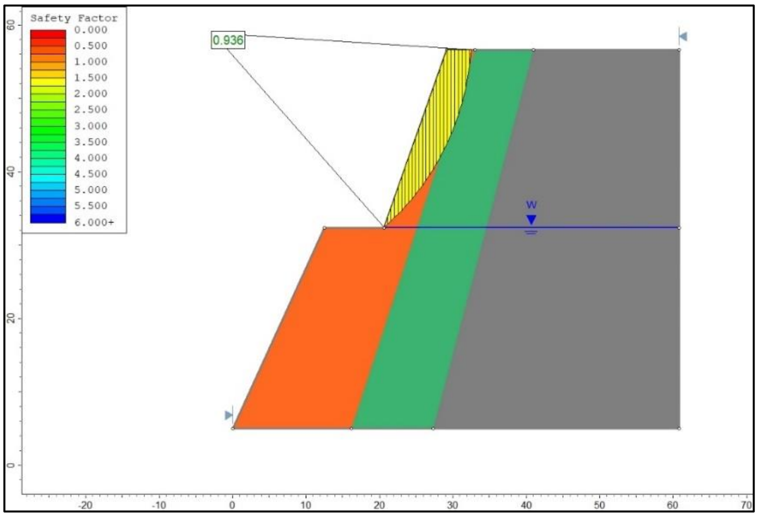

Figure 10. Landslide analysis.

The high potential for landslides on road slopes is caused by the discontinuity planes found on the slopes and the slope geometry that is not in accordance with the research of Loilatu & Iswandaru (2022) which proves the influence of slope geometry on landslides. In this study, slope stability analysis was carried out using geometry based on field surveys, which is an upper slope slope of 75 degrees with a road width of 10 meters and a lower slope slope of 65 degrees, which shows a very steep geometry, resulting in an FK value of 0.396 or <1.25 which indicates that the slope conditions are less stable and have the potential for landslides (Figure 10). This is in accordance with the results of mapping using GIS which on coordinate 844,083.917 (Easting) and 9,662,077.398 (Northing) shows that the area is an area with high landslide potential (Figure 9).

Conclusion

The results of the study showed that almost 85% of the research area is a high landslide potential area which is the Palopo–Luwu main road area, this was validated from laboratory test data which was then analyzed for slope stability showing an FK value <1.25, which is 0.936 and the actual condition of the slope in the field has collapsed.

Acknowledgements

This research was supported by the POP BIMA Research Grant (2024) from the Ministry of Education, Culture, Research, and Technology, Republic of Indonesia. The authors gratefully acknowledge the Department of Mining Engineering, University Andi Djemma, for providing laboratory facilities and technical assistance. We also thank the Luwu Regency Government for sharing geospatial data and the student research team for their contributions to field data collection.

Author Contributions

Anshar Abdullah Jawil provided conceptualization, funding acquisition, methodology, supervision, writing original draft. Kadek Nando Setiawan provided data curation, formal analysis (GIS/FEM), software, visualization, writing—review & editing. Both authors contributed equally to fieldwork, validation, and manuscript finalization.

Conflict of Interest

The authors declare no financial or personal conflicts of interest.

References

Brady, B. H. G., & Brown, E. (2006). *Rock Mechanics For Underground Mining*. Chapman and Hall.

Chen, W., & Zhang, S. (2021). GIS-based comparative study of Bayes network, Hoeffding tree and logistic model tree for landslide susceptibility modeling. *Catena*, 203, 105344. https://doi.org/10.1016/j.catena.2021.105344

Chen, X., Zhang, L., Chen, L., Li, X., & Liu, D. (2019). Slope stability analysis based on the Coupled Eulerian-Lagrangian finite element method. *Bulletin of Engineering Geology and the Environment*, 78(6), 4451–4463. https://doi.org/10.1007/s10064-018-1413-4

Cuomo, S., Di Perna, A., & Martinelli, M. (2021). Modelling the spatio-temporal evolution of a rainfall-induced retrogressive landslide in an unsaturated slope. *Engineering Geology*, 294, 106371. https://doi.org/10.1016/j.enggeo.2021.106371

Du, K., Li, X., Wang, S., Tao, M., Li, G., & Wang, S. (2021). Compression-shear failure properties and acoustic emission (AE) characteristics of rocks in variable angle shear and direct shear tests. *Measurement*, 183, 109814. https://doi.org/10.1016/j.measurement.2021.109814

Hoek, E., & Brown, E. T. (2019). The Hoek–Brown failure criterion and GSI – 2018 edition. *Journal of Rock Mechanics and Geotechnical Engineering*, 11(3), 445–463. https://doi.org/10.1016/j.jrmge.2018.

08.001

Huang, G., Zheng, M., & Peng, J. (2021). Effect of Vegetation Roots on the Threshold of Slope Instability Induced by Rainfall and Runoff. *Geofluids*, 2021(1), 6682113. https://doi.org/10.1155/2021/6682113

Jawil, A. A., & Pontus, A. J. (2023). Analisis Penurunan Muka Tanah (Subsidens) Menggunakan Metode Empirik Di Terowongan Penstock Sta 10+ 150 PLTA Kerinci Merangin, Kabupaten Kerinci, Provinsi Jambi. *Jurnal Teknologi Mineral FT Unmul*, 11(1), 26–33. http://dx.doi.org/10.30872/jtm.v11i1.11455

Khatun, M., Hossain, A. S., Sayem, H. M., Moniruzzaman, M., Ahmed, Z., & Rahaman, K. R. (2023). Landslide susceptibility mapping using weighted-overlay approach in Rangamati, Bangladesh. Earth Systems and Environment, https://doi.org/10.1007/s41748-022-00312-2

Li, D.-Q., Xiao, T., Cao, Z.-J., Phoon, K.-K., & Zhou, C.-B. (2016). Efficient and consistent reliability analysis of soil slope stability using both limit equilibrium analysis and finite element analysis. *Applied Mathematical Modelling*, 40(9), 5216–5229. https://doi.org/10.1016/j.apm.2015.11.044

Liu, Y., Deng, Z., & Wang, X. (2021). The effects of rainfall, soil type and slope on the processes and mechanisms of rainfall-induced shallow landslides. Applied Sciences, 11(24), 11652. https://doi.org/10.3390/app112411652

Loilatu, R., & Iswandaru, I. (2022). Analisis Kestabilan Lereng Andesit Menggunakan Metode FEM pada PT. X. *Jurnal Riset Teknik Pertambangan*, 2(1), 15–23. https://doi.org/10.29313/jrtp.v2i1.782

Nath, S. K., Sengupta, A., & Srivastava, A. (2021). Remote sensing GIS-based landslide susceptibility & risk modeling in Darjeeling–Sikkim Himalaya together with FEM-based slope stability analysis of the terrain. *Natural Hazards*, 108(3), 3271–3304. https://doi.org/10.1007/s11069-021-04823-5

Neamat, S., & Karimi, H. (2020). A systematic review of GIS-based landslide Hazard Mapping on Determinant Factors from International Databases. *2020 international conference on advanced science and engineering (ICOASE)*, 180–183. https://doi.org/10.1109/ICOASE51841.2020.9436611

Pawluszek-Filipiak, K., Oreńczak, N., & Pasternak, M. (2020). Investigating the effect of cross-modeling in landslide susceptibility mapping. *Applied Sciences*, 10(18), 6335. https://doi.org/10.3390/app10186335

Pilecka, E., Szwarkowski, D., Stanisz, J., & Blockus, M. (2022). Analysis of a landslide on a railway track using laser scanning and FEM numerical modelling. *Applied Sciences*, 12(15), 7574. https://doi.org/10.3390/app12157574

PU Regulation No.22 (2007). Kementerian Pekerjaan Umum dan Perumahan Rakyat, Indonesia.

Rawat, P. K., & Pant, B. (2023). Geoenvironmental GIS development to investigate Landslides and Slope Instability along Frontal zone of Central Himalaya. *Natural Hazards Research*, 3(2), 196–204. https://doi.org/10.1016/j.nhres.2023.03.005

Saleem, J., Ahmad, S. S., & Butt, A. (2020). Hazard risk assessment of landslide-prone sub-Himalayan region by employing geospatial modeling approach. *Natural Hazards*, 102(3), 1497–1514. https://doi.org/10.1007/s11069-020-03980-3

Simandjuntak, T. O., Rusmana, E, Suroso, S., & Supandjono, J. B. (2007). *Peta Geologi Lembar Malili*. Pusat Penelitian dan Pengembangan Geologi, Indonesia.

Susilo, A., Fitriah, F., Ayu Rachmawati, E. T., & Suryo, E. A. (2020). Analysis of landslide area of Tulung subdistrict, Ponorogo, Indonesia in 2017 using resistivity method. *Smart and Sustainable Built Environment*, 9(4), 341–360. https://doi.org/10.1108/SASBE-06-2019-0082

Wang, G., Chen, X., & Chen, W. (2020). Spatial prediction of landslide susceptibility based on GIS and discriminant functions. *ISPRS International Journal of Geo-Information*, 9(3), 144. https://doi.org/10.3390/ijgi9030144

Wyllie, D. C, & Mah, C. (2004). *Rock Slope Engineering Civil and Mining*, 4th Edition. CRC Press.